

Syntheses, crystal structures and catalytic properties of a series of lanthanide(III) bis(trimethylsilyl)amide chloride complexes: $[\{((\text{Me}_3\text{Si})_2\text{N})_2\text{Ln}(\mu'\text{-Cl})\text{Li}(\text{THF})_3\}(\mu\text{-Cl})]_2$, $[\{((\text{Me}_3\text{Si})_2\text{N})_2\text{Ln}(\mu'\text{-Cl})\text{Li}(\text{THF})_2\}(\mu_3\text{-Cl})]_2$ (Ln = Eu, Ho), and $[\{(\text{Me}_3\text{Si})_2\text{NLn}(\mu'\text{-Cl})_2\text{Li}(\text{THF})_2\}(\mu\text{-Cl})]_2$ (Ln = Nd, Sm, Eu, Ho, Yb)

Hong-Xi Li ^a, Qing-Feng Xu ^a, Jin-Xiang Chen ^a, Mei-Ling Cheng ^a, Yong Zhang ^a,
Wen-Hua Zhang ^a, Jian-Ping Lang ^{a,b,*}, Qi Shen ^a

^a Key Laboratory of Organic Synthesis of Jiangsu Province, School of Chemistry and Engineering, Suzhou University,
1 Shizi Street, Suzhou 215006, Jiangsu, PR China

^b State Key Laboratory of Organometallic Chemistry, Shanghai Institute of Organic Chemistry,
Chinese Academy of Sciences, Shanghai 200032, PR China

Received 24 May 2004; accepted 27 July 2004

Available online 11 September 2004

Abstract

Reactions of anhydrous lanthanide(III) trichloride (Ln = Nd, Sm, Eu, Ho, Yb) with one or two equiv. of $\text{LiN}(\text{SiMe}_3)_2$ in THF produced a family of lanthanide(III) bis(trimethylsilyl)amide chloride complexes: $[\{((\text{Me}_3\text{Si})_2\text{N})_2\text{Ln}(\mu'\text{-Cl})\text{Li}(\text{THF})_3\}(\mu\text{-Cl})]_2$ (**1**), $[\{((\text{Me}_3\text{Si})_2\text{N})_2\text{Ln}(\mu'\text{-Cl})\text{Li}(\text{THF})_2\}(\mu_3\text{-Cl})]_2$ (Ln = Eu (**2**); Ln = Ho (**3**)), and $[\{(\text{Me}_3\text{Si})_2\text{NLn}(\mu'\text{-Cl})_2\text{Li}(\text{THF})_2\}(\mu\text{-Cl})]_2$ (Ln = Nd (**4**); Ln = Sm (**5**); Ln = Eu (**6**); Ln = Ho (**7**); Ln = Yb (**8**)). On the other hand, reactions of the monosubstituted silylamido complexes $[\{(\text{Me}_3\text{Si})_2\text{NLn}(\mu'\text{-Cl})_2\text{Li}(\text{THF})_2\}(\mu\text{-Cl})]_2$ (Ln = Nd (**4**); Sm (**5**); Eu (**6**); Ho (**7**)) with 2 equiv. of $\text{LiN}(\text{SiMe}_3)_2$ in THF afforded the corresponding disubstituted complexes $[\{((\text{Me}_3\text{Si})_2\text{N})_2\text{Ln}(\mu'\text{-Cl})\text{Li}(\text{THF})_3\}(\mu\text{-Cl})]_2$ (Ln = Nd (**1**); Sm (**9**)) $[\{((\text{Me}_3\text{Si})_2\text{N})_2\text{Ln}(\mu'\text{-Cl})\text{Li}(\text{THF})_2\}(\mu_3\text{-Cl})]_2$ (Ln = Sm (**9**), Eu (**2**); Ho (**3**)). These complexes were characterized by melting point determination, elemental analysis and IR spectra. Single-crystal X-ray diffraction studies revealed that these compounds are chloride-bridged dimers, in which Ln metals in **1–3** display a distorted trigonal bipyramidal coordination geometry while those in **5**, **6** and **8** a distorted octahedral coordination geometry. Complexes **1–9** exhibited catalytic activity for the ring-opening polymerization of ϵ -caprolactone.

© 2004 Elsevier B.V. All rights reserved.

Keywords: Lanthanides; Bis(trimethylsilyl)amide; Structure; Catalysis; Synthesis

1. Introduction

In the past decades, lanthanide metals have been known to react with various amides to form lanthanide amide complexes. These complexes have attracted much

attention due to their diverse structures [1–7], their applications in catalysis [8] and the material science [9]. The bulky bis(trimethylsilyl)amido ligand $\text{N}(\text{SiMe}_3)_2^-$ was initially introduced to lanthanide chemistry [10] by Bradley in 1973. So far, a number of X-ray crystal structures of three-coordination lanthanide(III) amides $\text{Ln}[\text{N}(\text{SiMe}_3)_2]_3$ (Ln = Sc, Y, Ce, Nd, Eu, Dy, Yb) [11], tetracoordinate lanthanide(III) complexes $[(\text{Me}_3\text{Si})_2\text{N}]_3\text{Ln}(\mu\text{-Cl})\text{Li}(\text{THF})_3$ (Ln = Nd, Sm, Eu, Yb)

* Corresponding author. Tel.: +86 512 65213506; fax: + 86 512 65224783.

E-mail address: jplang@suda.edu.cn (J.-P. Lang).

[12], five-coordination lanthanide(III) compounds $[\{((\text{Me}_3\text{Si})_2\text{N})_2\text{Sm}(\mu'\text{-Cl})\text{Li}(\text{THF})_3\}(\mu\text{-Cl})]_2$ [13], $[(\mu\text{-Cl})\text{Ln}\{\text{N}(\text{SiMe}_3)_2\}_2(\text{THF})]_2$ (Ln = Nd [14], Gd, and Yb [15]), and lanthanide(II) complexes $[(\text{Me}_3\text{Si})_2\text{N}_2\text{Sm}(\text{THF})_2]$, $[\{(\text{Me}_3\text{Si})_2\text{N}\}\text{Sm}(\mu\text{-I})(\text{DME})(\text{THF})_2]_2$ [16], $\text{NaM}[\text{N}(\text{SiMe}_3)_2]_3$ (M = Yb, Eu) [17] have been reported.

On the other hand, the ring-opening polymerization (ROP) of lactones provides a convenient route to biodegradable and biocompatible polyesters, which are of great interest for various practical applications [18–21]. In recent years, a series of Ln(III) compounds such as yttrium isopropoxide, lanthanide alkoxides, lanthanide hydride (or alkyl) and samarium(II) derivatives [22–26] were reported to initiate the ROP of lactones. However, only a few of the lanthanide amides, e.g., three-coordination compounds $\text{Y}[\text{N}(\text{SiMe}_3)_2]_3$ [26], $\text{Sm}[\text{N}(\text{SiMe}_3)_2]_3$, $[\{\text{N}(\text{SiMe}_3)_2\}_2\text{YbN}(\text{SiMe}_3)(\text{SiMe}_2)(\text{CH}_2\text{Na})(\text{THF})_3]$, five-coordination compounds $[\text{Sm}\{\text{N}(\text{SiMe}_3)_2\}_2(\mu\text{-Cl})(\text{THF})]_2$, $[\text{Sm}\{\text{N}(\text{SiMe}_3)_2\}_2(\mu\text{-Br})(\text{THF})]_2$ and lanthanide(II) complex $\text{Sm}[\text{N}(\text{SiMe}_3)_2]_2(\text{THF})_2$ [27] were found to be effective catalyst for the ROP of lactones. There was not much discussion about the relation between the catalytic properties and the structure of the lanthanide complexes (e.g., coordination number) [26,27].

We are currently interested in the preparation and catalytic activity of lanthanide silylamido complexes, and are curious about whether the activity of these complexes initiating the ROP of ϵ -caprolactone depends on the coordination number of the metals. Therefore we carried out reactions of anhydrous LnCl_3 (Ln = Nd, Sm, Eu, Ho, Yb) with one or two equiv. of $\text{LiN}(\text{SiMe}_3)_2$ in THF, and a set of lanthanide(III) bis(trimethylsilyl)amide chloride complexes $[\{((\text{Me}_3\text{Si})_2\text{N})_2\text{Nd}(\mu'\text{-Cl})\text{Li}(\text{THF})_3\}(\mu\text{-Cl})]_2$ (**1**), $[\{((\text{Me}_3\text{Si})_2\text{N})_2\text{Ln}(\mu'\text{-Cl})\text{Li}(\text{THF})_2\}(\mu_3\text{-Cl})]_2$ (Ln = Eu (**2**); Ln = Ho (**3**)), and $[\{(\text{Me}_3\text{Si})_2\text{NLn}(\mu'\text{-Cl})_2\text{Li}(\text{THF})_2\}(\mu\text{-Cl})]_2$ (Ln = Nd (**4**); Ln = Sm (**5**); Ln = Eu (**6**); Ln = Ho (**7**); Ln = Yb (**8**)) were isolated therefrom. Compounds **1–3** and **5**, **6**, **8** were determined by X-ray crystallography. Furthermore, we found that reactions of the monosubstituted silylamido complexes of lanthanide **4–7** with two equiv. of $\text{LiN}(\text{SiMe}_3)_2$ could be easily turned into the corresponding disubstituted ones **1–3** and the known complex $[\{((\text{Me}_3\text{Si})_2\text{N})_2\text{Sm}(\mu'\text{-Cl})\text{Li}(\text{THF})_3\}(\mu\text{-Cl})]_2$ (**9**). In addition, complexes **1–9** were confirmed to be catalytic activity in the ROP of ϵ -caprolactone. Herein we report the isolation, structural characterization and catalytic property of **1–9**.

2. Results and discussion

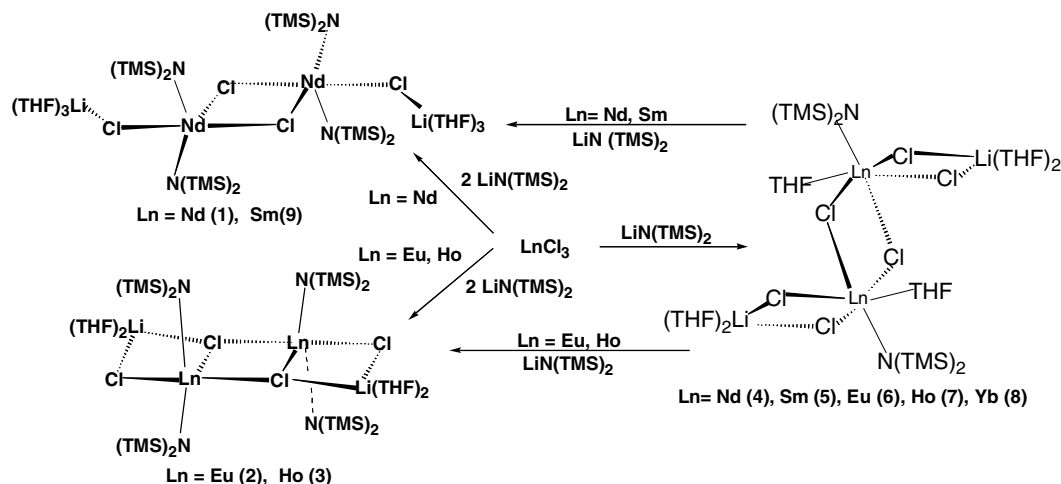
2.1. Synthesis

The disubstituted silylamido complexes of lanthanide are known to be isolated from reaction of LnCl_3 with

$\text{LiN}(\text{SiMe}_3)_2$ [13] or $\text{NaN}(\text{SiMe}_3)_2$ [14]. For instance, reaction of SmCl_3 with 2 equiv. of $\text{LiN}(\text{SiMe}_3)_2$ in THF formed the complex $[\{((\text{Me}_3\text{Si})_2\text{N})_2\text{Sm}(\mu'\text{-Cl})\text{Li}(\text{THF})_3\}(\mu\text{-Cl})]_2$ [13], while treatment of NdCl_3 or CeCl_3 with 2 equiv. $\text{NaN}(\text{SiMe}_3)_2$ in THF at 80 °C yield $[\text{Ln}\{\text{N}(\text{SiMe}_3)_2\}_2(\mu\text{-Cl})(\text{THF})]_2$ (Ln = Nd, Ce) [14]. In our case, treatment of solid $\text{LiN}(\text{SiMe}_3)_2$ with a suspension of anhydrous NdCl_3 in THF at 193 K followed by slowly warming the mixture up to ambient temperature led to a light blue solution. After removal of all the volatile species in vacuo, the residue was extracted with hot *n*-hexane and the insoluble LiCl precipitate was filtered. The blue filtrate was allowed to stand at room temperature for several days, forming blue crystals of $[\{((\text{Me}_3\text{Si})_2\text{N})_2\text{Nd}(\mu'\text{-Cl})\text{Li}(\text{THF})_3\}(\mu\text{-Cl})]_2$ (**1**) in 67% yield (Scheme 1). When we carried out the reactions of anhydrous EuCl_3 or HoCl_3 in THF with 2 equiv. of $\text{LiN}(\text{SiMe}_3)_2$ at ambient temperature, $[\{((\text{Me}_3\text{Si})_2\text{N})_2\text{Ln}(\mu'\text{-Cl})\text{Li}(\text{THF})_2\}(\mu_3\text{-Cl})]_2$ (Ln = Eu (**2**); Ln = Ho (**3**)) was obtained in 73% (**2**) or 53% (**3**) yield in a similar workup to that used in the isolation of **1**. On the other hand, reactions of anhydrous LnCl_3 (Ln = Nd; Sm; Eu; Ho; Yb) with equimolar $\text{LiN}(\text{SiMe}_3)_2$ in THF at room temperature followed by standard workups afforded $[\{(\text{Me}_3\text{Si})_2\text{NLn}(\mu'\text{-Cl})_2\text{Li}(\text{THF})_2\}(\mu\text{-Cl})]_2$ (Ln = Nd (**4**); Ln = Sm (**5**); Ln = Eu (**6**); Ln = Ho (**7**); Ln = Yb (**8**)) in moderate yields. Interestingly, the disubstituted silylamido complexes can be easily formed in relatively higher yield, subject to addition of two equiv. of $\text{LiN}(\text{SiMe}_3)_2$ into the monosubstituted silylamido complexes. For example, treatment of **5** with two equiv. of $\text{LiN}(\text{SiMe}_3)_2$ in THF gave rise to the known complex $[\{((\text{Me}_3\text{Si})_2\text{N})_2\text{Sm}(\mu'\text{-Cl})\text{Li}(\text{THF})_3\}(\mu\text{-Cl})]_2$ (**9**) in 69% yield. However, reaction of the disubstituted complexes with one equiv. LnCl_3 (Ln = Nd, Sm, Eu, Ho) did not lead to the formation of the corresponding monosubstituted ones. Complexes **1–9** are highly air- and moisture-sensitive, and are readily soluble in DME, THF, and toluene, and slightly soluble in *n*-hexane. Elemental analyses of **1–9** are consistent with the formulas. The crystal structures of **1**, **2**, **3**, **5**, **6** and **8** were finally confirmed by X-ray crystallography.

2.2. Molecular structure of $[\{((\text{Me}_3\text{Si})_2\text{N})_2\text{Nd}(\mu'\text{-Cl})\text{Li}(\text{THF})_3\}(\mu\text{-Cl})]_2$ (**1**)

Compound **1** crystallizes in the triclinic space group $P\bar{1}$ and the asymmetric unit contains one-half of the discrete molecule $[\{((\text{Me}_3\text{Si})_2\text{N})_2\text{Nd}(\mu'\text{-Cl})\text{Li}(\text{THF})_3\}(\mu\text{-Cl})]_2$. The molecular structure of **1** is showed in Fig. 1 and its selected bond distances and angles are listed in Table 1. Compound **1** consists of two $\{((\text{Me}_3\text{Si})_2\text{N})_2\text{Nd}(\mu'\text{-Cl})\text{Li}(\text{THF})_3\}$ units interconnected by two $\mu\text{-Cl}$ atoms, forming a dimeric structure with a crystallographic center of symmetry on the midpoint of the Nd(1) and Nd(1') atoms. The structure closely resembles that of its samarium analogue $[\{((\text{Me}_3\text{Si})_2\text{N})_2\text{Sm}(\mu'\text{-Cl})\text{Li}(\text{THF})_3\}]$



Scheme 1.

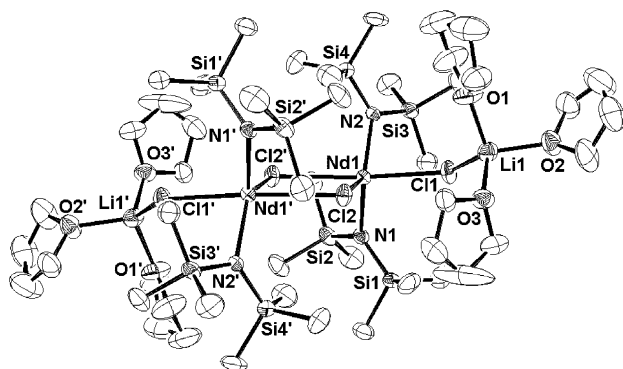


Fig. 1. Molecular structure of $\{[(\text{Me}_3\text{Si})_2\text{N})_2\text{Nd}(\mu\text{-Cl})\text{Li}(\text{THF})_3](\mu\text{-Cl})_2\}$ (**1**) with 50% thermal ellipsoids. All hydrogen atoms are omitted for clarity.

$(\mu\text{-Cl})_2$ [13] and $[(\mu\text{-Cl})\text{Nd}\{\text{N}(\text{SiMe}_3)_2\}_2(\text{THF})_2]$ [14]. In the structure of **1**, either Nd(1) or Nd(1') atom adopts a distorted bipyramidal coordination geometry. As the $\text{N}(1)\text{--Nd}(1)\text{--N}(2)$ angles ($116.59(10)^\circ$) is apparently narrower than the $\text{Cl}(1)\text{--Nd}(1)\text{--Cl}(2')$ angle ($156.75(2)^\circ$), the five-coordinated Nd atom in **1** can be better described as pseudo trigonal bipyramidal in which apical positions are occupied by Cl(1) and Cl(2'). In the Nd_2Cl_2 rhomb, the two bridging chlorine atoms are unsymmetrically located between the neodymium atoms with Nd(1) $\text{--}\mu\text{-Cl}(2)$ of 2.8337(8) Å and Nd(1) $\text{--}\mu\text{-Cl}(2')$ of 2.8580(8) Å. Their mean bond length (2.8458 Å) is 0.08 Å longer than that of the Nd(1) $\text{--}\mu\text{-Cl}(1)$ and Nd(1') $\text{--}\mu\text{-Cl}(1')$ bonds (2.7689 Å), but slightly shorter than that found in $[(i\text{Pr})\text{TP}\{\text{NdCl}(\text{THF})_2\}_2((i\text{Pr})\text{TP})]$ (1,3-bis(2-propylamino)troponimate) (2.887 Å) [28]. The Nd–N bond distances (2.305(3)–2.313(5) Å) are shorter than those observed in $[(i\text{Pr})\text{TP}\{\text{NdCl}(\text{THF})_2\}_2]$ (2.38(2)–2.52(2) Å) [28], and $[\text{Nd}(\text{tBu}_2\text{pz})_3(\mu\text{-DME})]_n$ (tBu_2pz = 3,5-bi-*tert*-butylpyrazolate) (2.390(5)–2.499(7) Å) [29]. Each Li atom is coordinated by a μ' -Cl and three THF molecules, form-

Table 1

Selected bond lengths (Å) and angles ($^\circ$) of **1**

Nd(1)–Cl(1)	2.7689(11)	Li(1)–Cl(1)	2.336(8)
Nd(1)–Cl(2)	2.8337(8)	Li(1)–O(1)	1.923(7)
Nd(1)–Cl(2')	2.8580(8)	Li(1)–O(2)	1.946(8)
Nd(1)–N(1)	2.305(3)	Li(1)–O(3)	1.942(9)
Nd(1)–N(2)	2.313(3)		
Cl(1)–Nd(1)–Cl(2)	84.80(3)	Cl(1)–Nd(1)–N(1)	105.17(7)
Cl(1)–Nd(1)–N(2)	88.71(8)	Cl(1)–Nd(1)–Cl(2')	156.75(2)
Cl(2)–Nd(1)–Cl(2')	73.44(3)	Cl(2)–Nd(1)–N(1)	112.60(7)
Cl(2)–Nd(1)–N(2)	130.35(6)	N(1)–Nd(1)–N(2)	116.59(10)
N(1)–Nd(1)–Cl(2')	90.97(7)	N(2)–Nd(1)–Cl(2')	99.05(7)
Cl(1)–Li(1)–O(1)	111.8(4)	Cl(1)–Li(1)–O(2)	116.3(2)
Cl(1)–Li(1)–O(3)	109.8(4)	O(1)–Li(1)–O(2)	102.9(4)
O(1)–Li(1)–O(3)	110.7(3)	O(2)–Li(1)–O(3)	105.0(4)
Li(1)–Cl(1)–Nd(1)	136.12(13)		

ing a distorted tetrahedral coordination geometry. The mean Li–O and Li– μ' -Cl bond lengths are 1.937 Å and 2.336(8) Å, respectively, which are comparable to those of the corresponding ones in $[(\text{Me}_3\text{Si})_2\text{N}]_3\text{Nd}(\mu\text{-Cl})\text{Li}(\text{THF})_3$ (Li–O = 1.91 Å, Li– $\mu\text{-Cl}$ = 2.33 Å) [12]. Noteworthy, the Nd(1) $\text{--}\mu'\text{-Cl}(1)\text{--Li}(1)$ angle of $136.12(13)^\circ$ in both $[(\text{Me}_3\text{Si})_2\text{N}]_2\text{Nd}(\mu'\text{-Cl})\text{Li}(\text{THF})_3$ units of **1** is 39° smaller than that in mononuclear complex $[(\text{Me}_3\text{Si})_2\text{N}]_3\text{Nd}(\mu\text{-Cl})\text{Li}(\text{THF})_3$ ($175.4(6)^\circ$) [12], which may be due to steric hindrance caused by four bulky $\text{N}(\text{SiMe}_3)_2$ ligands when the two units are linked by two Nd– $\mu\text{-Cl}$ –Nd bridges.

2.3. Molecular structures of $[\{((\text{Me}_3\text{Si})_2\text{N})_2\text{Ln}(\mu'\text{-Cl})\text{Li}(\text{THF})_2\}(\mu_3\text{-Cl})_2]$ ($\text{Ln} = \text{Eu}$ (**2**); $\text{Ln} = \text{Ho}$ (**3**))

Compound **2** crystallizes in the triclinic space group $P\bar{1}$ and the asymmetric unit contains one-half of the discrete molecule $[\{((\text{Me}_3\text{Si})_2\text{N})_2\text{Eu}(\mu'\text{-Cl})\text{Li}(\text{THF})_2\}(\mu_3\text{-Cl})_2]$ (**2**). However, **3** crystallizes in the monoclinic space group $P2_1/n$ and the asymmetric unit contains one-half of the

discrete molecule $[\{(Me_3Si)_2N\}_2Ho(\mu'-Cl)Li(THF)_2](\mu_3-Cl)_2$ (**3**). As the molecular structures of **2** and **3** are very similar, only that of **2** is shown in Fig. 2. Their selected bond distances and angles are listed in Table 2. Compounds **2** and **3** also adopt a dimeric structure in which two $\{(Me_3Si)_2N\}_2Ln(\mu'-Cl)Li(THF)_2$ moieties are symmetrically bridged by two μ_3-Cl atoms. A crystallographic inversion center is located on the midpoint of the two Ln centers. In the structure of **2** or **3**, the Ln center is coordinated by two μ_3-Cl , one $\mu'-Cl$ and two N atoms to form a severely distorted trigonal bipyramidal geometry. Three chloride atoms surrounding the Ln atom sit on the equatorial plane while two $N(SiMe_3)_2$ ligands are located on the axial positions. The $Eu-\mu_3-Cl$, $Eu-\mu'-Cl$ and $Eu-N$ bond distances in **2** are smaller than those of the $Ho-\mu_3-Cl$, $Ho-\mu'-Cl$ and $Ho-N$ bonds in **3**, which is consistent with the fact that Eu has a shorter ionic radius than Ho. The existence of the $Ln-\mu_3-Cl$ bonds in **2** and **3** are uncommon in Eu and Ho chloride complexes [30]. The mean $Ln-\mu-Cl$ bond length, 2.6806 Å (**2**) or 2.625 Å (**3**), is shorter than those in $[Eu(NR_2)_3(\mu-Cl)Li(THF)_3]$ ($R_2 = -SiMe_2CH_2CH_2SiMe_2-$) ($Eu-\mu-Cl = 2.657$ Å) [31] and in $(Cp_2HoCl)_2$ (2.673 Å) [32]. The average $Ln-N$ bond distances of **2** and **3** are 2.257 and 2.206 Å, which are close to those of the corresponding ones in $[Ln(NR_2)_3(\mu-Cl)Li(L_3)]$ ($R_2 = -SiMe_2CH_2CH_2SiMe_2-$) (2.254 Å for $Ln = Eu$, $L = THF$; 2.221 Å for $Ln = Ho$, $L = Et_2O$) [31]. The tetrahedral coordination sphere of each Li atom is completed by one $\mu'-Cl$, one μ_3-Cl and two O atoms from THF molecules. The mean $Li-\mu'-Cl$ bond distance (2.361(7) Å (**2**) and 2.33(1) Å (**3**)) is comparable to that in **1**, but longer than that in $[(iPr_2N)_2SmCl_3\{Li(TMEDA)\}_2]$ (2.285 Å) [33]. The mean $Li-\mu_3-Cl$ bond length (2.509(6) Å (**2**) and 2.54(2) Å (**3**)) is longer than that in $[(iPr_2N)_2SmCl_3\{Li(TMEDA)\}_2]$ (2.335 Å) [33]. The mean $Li-O$ bond length (1.909 Å (**2**) and 1.91 Å (**3**)) is shorter than that in **1**.

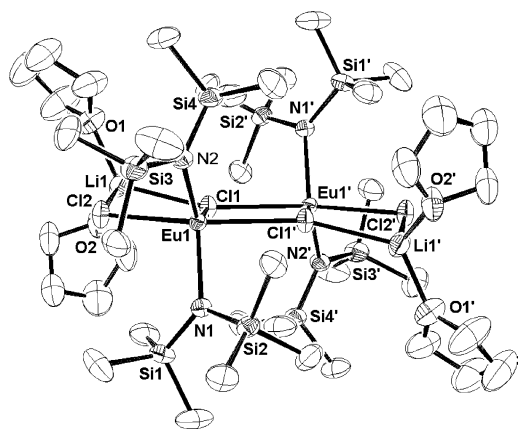


Fig. 2. Molecular structure of $[\{(Me_3Si)_2N\}_2Eu(\mu'-Cl)Li(THF)_2](\mu_3-Cl)_2$ (**3**) with 50% thermal ellipsoids. All hydrogen atoms are omitted for clarity.

Table 2
Selected bond lengths (Å) and angles (°) of **2** and **3**

2		3	
Eu(1)–Cl(1)	2.8515(8)	Ho(1)–Cl(1)	2.788(2)
Eu(1)–Cl(2)	2.6806(8)	Ho(1)–Cl(2)	2.625(2)
Eu(1)–Cl(1')	2.8550(6)	Ho(1)–Cl(1')	2.774(2)
Eu(1)–N(1)	2.246(2)	Ho(1)–N(1)	2.202(6)
Eu(1)–N(2)	2.268(3)	Ho(1)–N(2)	2.202(6)
Li(1)–Cl(1)	2.509(6)	Li(1)–Cl(1)	2.54(2)
Li(1)–Cl(2)	2.361(7)	Li(1)–Cl(2')	2.33(2)
Li(1)–O(1)	1.917(6)	Li(1)–O(1)	1.91(2)
Li(1)–O(2)	1.901(9)	Li(1)–O(2)	1.91(2)
Cl(1)–Eu(1)–Cl(2)	77.71(2)	Cl(1)–Ho(1)–Cl(2)	153.70(7)
Cl(1)–Eu(1)–Cl(1')	72.36(2)	Cl(1)–Ho(1)–Cl(1')	73.73(5)
Cl(1)–Eu(1)–N(1)	114.01(7)	Cl(1)–Ho(1)–N(1)	100.8(2)
Cl(1)–Eu(1)–N(2)	127.14(6)	Cl(1)–Ho(1)–N(2)	92.7(2)
Cl(2)–Eu(1)–N(1)	101.18(7)	Cl(2)–Ho(1)–N(1)	91.3(2)
Cl(2)–Eu(1)–N(2)	89.27(7)	Cl(2)–Ho(1)–N(2)	102.1(2)
Cl(2)–Eu(1)–Cl(1')	150.06(2)	Cl(2)–Ho(1)–Cl(1')	80.34(6)
N(1)–Eu(1)–N(2)	118.76(8)	N(1)–Ho(1)–N(2)	118.2(2)
N(1)–Eu(1)–Cl(1')	91.97(6)	N(1)–Ho(1)–Cl(1')	127.3(2)
N(2)–Eu(1)–Cl(1')	107.88(7)	N(2)–Ho(1)–Cl(1')	114.4(2)
Cl(1)–Li(1)–Cl(2)	90.9(2)	Cl(1)–Li(1)–Cl(2')	91.4(5)
Cl(1)–Li(1)–O(1)	128.4(3)	Cl(1)–Li(1)–O(1)	125.1(8)
Cl(1)–Li(1)–O(2)	105.6(3)	Cl(1)–Li(1)–O(2)	105.5(7)
Cl(2)–Li(1)–O(1)	102.6(3)	Cl(2')–Li(1)–O(1)	107.3(8)
Cl(2)–Li(1)–O(2)	117.3(3)	Cl(2')–Li(1)–O(2)	118.5(8)
O(1)–Li(1)–O(2)	111.2(4)	O(1)–Li(1)–O(2)	109.0(8)

2.4. Molecular structures of $[\{(Me_3Si)_2N\}_2Ln(\mu'-Cl)_2Li(THF)_2](\mu-Cl)_2$ ($Ln = Sm$ (**5**); $Ln = Eu$ (**6**); $Ln = Yb$ (**8**))

Being crystallized in the triclinic space group $P\bar{1}$, the asymmetric unit for either **5** or **6** or **8** consists of one half of the discrete molecule $[\{(Me_3Si)_2N\}_2Ln(\mu'-Cl)_2Li(THF)_2](\mu-Cl)_2$ ($Ln = Sm$ (**5**); $Ln = Eu$ (**6**); $Ln = Yb$ (**8**)). Their cell parameters are essentially identical, and so are their molecular structures. Therefore only the perspective view of $[\{(Me_3Si)_2N\}_2Sm(\mu'-Cl)_2Li(THF)_2](\mu-Cl)_2$ is shown in Fig. 3. The bond lengths and angles for **5**, **6** and **8** are compared in Table 3. X-ray diffraction analysis confirmed that **5** or **6**, **8** is a dimeric structure which is composed of two $\{(Me_3Si)_2N\}_2Ln(\mu'-Cl)_2Li(THF)_2$ units linked by two $\mu-Cl$ atoms. An inversion center resides at the middle of the two Ln metals. Each Sm or Eu, Yb atom in **5**, **6**, and **8** adopts a distorted octahedral geometry defined by four chloride atoms, a nitrogen atom of amide group and an oxygen atom from THF molecule. The mean $Ln-\mu'-Cl(1)$ and $Ln-\mu'-Cl(2)$ bond distances are slightly shorter than those of $Ln-\mu-Cl(3)$ and $Ln-\mu-Cl(3')$ bonds. The average $Sm-\mu-Cl$ bond distance (2.754 Å) is shorter than those observed in $[(Cy_2N)_2Sm(\mu-Cl)(THF)]_2$ (2.800 Å) and $[(iPr_2N)_2SmCl_3\{Li(TMEDA)\}_2]$ (2.802 Å) [33]. The average $Eu-\mu-Cl$ bond distance (2.741 Å) is longer than those observed in $[(Me_3Si)_2N]_3Eu(\mu-Cl)Li(THF)_3$ (2.650(2) Å) [12]. The mean $Yb-\mu-Cl$ bond length of 2.656 Å is

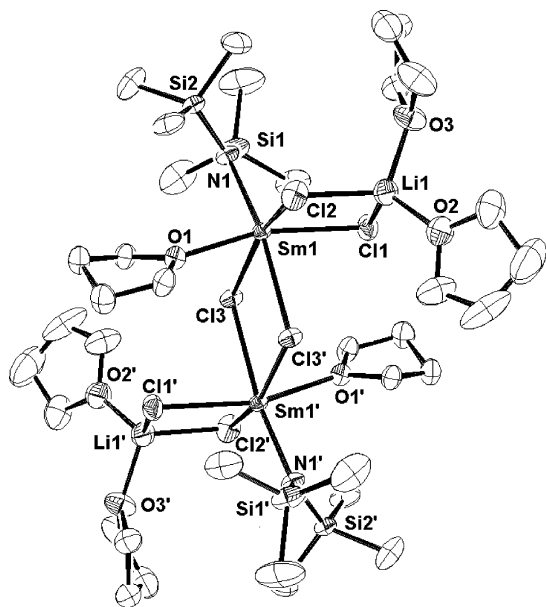


Fig. 3. Molecular structure of $[(\text{Me}_3\text{Si})_2\text{NSm}(\mu'\text{-Cl})_2\text{Li}(\text{THF})_2](\mu\text{-Cl})_2$ (**5**) with 50% thermal ellipsoids. All hydrogen atoms are omitted for clarity.

shorter than that found in $\{[(i\text{Pr})\text{TP}]\text{YbCl}\}_2$ ($(i\text{Pr})\text{TP}$ = 1,3-bis(2-isopropylamino)troponimate) (2.714 Å) [28]. The Ln–N and Ln–O bond distances decrease along with the ionic radius in the order of $\text{Yb} < \text{Eu} < \text{Sm}$. The mean Ln–N bond length, 2.284 Å (**5**) or 2.199 Å (**8**) is comparable to those reported in $\text{Cp}_2^*\text{SmN}(\text{SiMe}_3)_2$ (Sm–N = 2.301 Å) [34], $(S)\text{-Me}_2\text{Si}(\text{Me}_4\text{Cp})[(+)\text{-neomenthylCp}]\text{SmN}(\text{SiMe}_3)_2$ (Sm–N = 2.300 Å) [35], and $\text{Yb}(\text{NR}_2)_3(\mu\text{-Cl})\text{Li}(\text{Et}_2\text{O})_3$ ($\text{R}_2 = \text{-SiMe}_2\text{CH}_2\text{CH}_2\text{SiMe}_2\text{-}$) (Yb–N = 2.183 Å) [31]. However, the Eu–N bond length of 2.281(5) Å in **6** is shorter than that reported in $[(\text{Me}_3\text{Si})_2\text{N}]_3\text{Eu}(\mu\text{-Cl})\text{Li}(\text{THF})_3$ [12]. The average Ln–O bond distance, 2.421 Å (**5**) or 2.409(6) Å (**6**), 2.313 Å (**8**), is shorter than those in $[(\text{Cy}_2\text{N})_2\text{Sm}(\mu\text{-Cl})(\text{THF})_2]$ (Sm–O = 2.471 Å) [33] and $[(\text{Me}_3\text{Si})_2\text{N}]_2\text{Yb}(\mu\text{-Cl})(\text{THF})_2$ (Yb–O = 2.351 Å) [16], $[(\text{THF})_3\text{Eu}(\mu\text{-SPh})_2(\mu_3\text{-SPh})\text{Zn}(\text{SPh})_2] \cdot \text{THF}$ [36] (2.568 Å). The Cl(1)–Ln–Cl(2) angle in the planar “ LnCl_2Li ” rhomb, 83.02(3)° for **5**, 83.27(7)° for **6**, and 84.92(6)° for **8**, is larger than the Cl(3)–Ln–Cl(3') angle (77.08(2)° for **5**, 77.11(5)° for **6**, and 77.33(4)° for **8**) in the Ln_2Cl_2 rhomb. Each Li atom is coordinated by two $\mu'\text{-Cl}$ and two O atoms from THF molecules, forming a distorted tetrahedral geometry. The mean Li– $\mu'\text{-Cl}$ bond distance, 2.353 Å for **5**, 2.35 Å for **6**, and 2.36 Å for **8**, is close to that in **1**. The mean Li–O length (1.90 Å in **5**, **6** and **8**) is slightly shorter than that in **1**, but comparable to those in **2** and **3**.

2.5. ROP of ϵ -caprolactone

It has been reported that some lanthanide complexes of bis(trimethylsilyl)amide are effective catalysts in the

Table 3

Selected bond lengths (Å) and angles (°) of **5**, **6** and **8**

	5 (Ln = Sm)	6 (Ln = Eu)	8 (Ln = Yb)
Ln(1)–Cl(1)	2.7017(11)	2.687(2)	2.602(2)
Ln(1)–Cl(2)	2.6928(8)	2.681(2)	2.597(1)
Ln(1)–Cl(3)	2.7276(7)	2.878(2)	2.789(1)
Ln(1)–Cl(3')	2.8937(7)	2.718(2)	2.635(1)
Ln(1)–O(1)	2.421(3)	2.409(6)	2.313(5)
Ln(1)–N(1)	2.284(2)	2.281(5)	2.199(4)
Li(1)–Cl(1)	2.359(7)	2.35(1)	2.34(1)
Li(1)–Cl(2)	2.347(9)	2.35(2)	2.37(2)
Li(1)–O(2)	1.905(7)	1.90(1)	1.90(1)
Li(1)–O(3)	1.904(7)	1.91(1)	1.89(1)
Cl(1)–Ln(1)–Cl(2)	83.02(3)	83.27(7)	84.92(6)
Cl(1)–Ln(1)–Cl(3)	99.31(3)	82.53(6)	83.41(5)
Cl(1)–Ln(1)–Cl(3')	82.35(3)	99.02(6)	97.08(5)
Cl(2)–Ln(1)–Cl(3)	159.06(3)	82.78(5)	83.43(4)
Cl(2)–Ln(1)–Cl(3')	82.67(2)	159.23(6)	160.28(5)
Cl(3)–Ln(1)–Cl(3')	77.08(2)	77.11(5)	77.33(4)
Cl(1)–Ln(1)–O(1)	160.73(5)	161.0(1)	163.3(1)
Cl(2)–Ln(1)–O(1)	88.35(5)	88.2(1)	87.9(1)
Cl(3)–Ln(1)–O(1)	82.85(5)	79.5(1)	80.8(1)
Cl(3')–Ln(1)–O(1)	79.48(5)	83.2(1)	84.7(1)
Cl(1)–Ln(1)–N(1)	105.42(8)	104.9(2)	102.7(2)
Cl(2)–Ln(1)–N(1)	102.33(6)	102.4(1)	102.2(1)
Cl(3)–Ln(1)–N(1)	97.12(6)	171.3(2)	172.0(1)
Cl(3')–Ln(1)–N(1)	171.11(8)	97.0(1)	96.6(1)
N(1)–Ln(1)–O(1)	93.22(10)	93.5(2)	93.6(2)
Cl(2)–Li(1)–Cl(1)	98.9(3)	98.6(5)	96.4(4)
O(2)–Li(1)–O(3)	108.9(4)	109.2(7)	108.8(6)
Cl(1)–Li(1)–O(2)	117.3(3)	117.7(7)	119.2(6)
Cl(1)–Li(1)–O(3)	107.2(3)	108.0(6)	108.5(6)
Cl(2)–Li(1)–O(2)	113.3(4)	112.3(7)	111.5(6)
Cl(2)–Li(1)–O(3)	110.8(4)	110.7(7)	112.2(6)

ROP of ϵ -caprolactone [27]. We found that complexes **1–9** were also able to catalyze the ROP of ϵ -caprolactone in toluene at ambient temperature. When the polymerization was performed in toluene, a highly viscous product was observed to form in a few minutes in case of **1–3** and **9** and within 1 h in the case of **4–8**. After the resulting polymer was quenched by the addition of 1 M HCl in EtOH, the poly(ϵ -caprolactone) was isolated as white solids and characterized by gel permeation chromatography. As shown in Table 4, the yield of the poly(ϵ -caprolactone) was higher and the molecular weight distribution turned broader with longer reaction time, as was observed for the ROP of lactones initiated by other rare earth based initiators [24,37]. For instance, when **1** was used as a catalyst and the [monomer]/[cat.] mol ratio reached 800, the yield was 19% in 10 min at 298 K and the molecular weight distribution was 1.21. However, the yield became as high as 99% in 2 h and the molecular weight distribution got broader ($M_w/M_n = 1.91$). The polymerization systems in this paper gave high molecular weight polymers ($M_n > 10^4$). Using **1–3** and **9** (coordination number five) as a catalyst gave yields as high as 99% in 2 h at 298 K. Intriguingly, when using divalent samarium amides

Table 4
Polymerization of ϵ -caprolactone catalyzed by complexes **1–9**

Entry	Catalyst	Temp (K)	Time	[monomer]/[cat]	Yield	$M_n (\times 10^4)$ (g/mol)	$M_w (\times 10^4)$ (g/mol)	M_w/M_n
1	1	298	10 min	400	35	2.01	3.86	1.18
2	1	298	10 min	800	19	2.27	2.76	1.21
3	1	298	2 h	800	99	5.11	9.76	1.91
4	2	298	10 min	400	43	3.16	3.94	1.24
5	2	298	10 min	800	23	1.94	2.44	1.25
6	2	298	2 h	800	99	2.03	4.10	2.02
7	3	298	10 min	400	34	3.37	4.23	1.25
8	3	298	10 min	800	25	2.13	2.57	1.20
9	3	298	2 h	800	99	1.05	2.25	2.13
10	4	298	2 h	800	61	5.23	9.78	1.87
11	4	298	10 min	400	4	–	–	–
12	5	298	2 h	800	55	5.82	10.65	1.83
13	6	298	2 h	800	51	6.14	11.97	1.95
14	7	298	2 h	800	50	6.89	12.95	1.88
15	8	298	2 h	800	52	7.35	14.06	1.90
16	9	298	2 h	800	99	5.08	9.38	1.84

$[(\text{Me}_3\text{Si})_2\text{N}]_2\text{Sm}(\text{THF})_2$ [27] as catalysts in ROP of ϵ -caprolactone, the high yields were obtained in a few minutes, but their polymerization was attested by broad molecular weight distribution ($M_w/M_n > 2.6$). This is probably due to their low oxidation state and more open coordination environment around the Sm atom (coordination number four). Complexes **1–3** and **9** shown poorer catalytic activity than the compound $[(\mu\text{-Cl})\text{Sm}\{\text{N}(\text{SiMe}_3)_2\}_2(\text{THF})]_2$, which may be attributed to the effect of the attached “ $\text{CLi}(\text{THF})_x$ ” ($x = 2$ or 3) species. The homoleptic tris(amide) $\text{Sm}[\text{N}(\text{SiMe}_3)_2]_3$ was also found to polymerize ϵ -caprolactone and showed higher catalytic activity than complexes **1–9**. This may be due to the monodentate nature of ligands and the absence of an inert spectator ligand [26a]. Complexes **4–7** showed even poorer catalytic activity than the corresponding disubstituted complexes **1–3** and **9** under the same condition, which might be ascribed to the fact that **4–7** have a less open coordination environment around the Ln metal (coordination number six) than **1–3** and **9**. However, the molecular weight of polymers formed by compounds **4–7** were generally larger than those catalyzed by the corresponding disubstituted complexes **1–3** and **9**. For example, when **1** was used as a catalyst, the yield was 99% in 2 h at 298 K and the molecular weight M_n was 5.11×10^4 g/mol over [monomer]/[cat.] mol ratio of 800:1, while under the same conditions **4** only gave 61% yield and the molecular weight M_n was 5.23×10^4 g/mol.

3. Conclusion

In this paper, we have demonstrated that 1:1 or 1:2 reactions of LnCl_3 with $\text{LiN}(\text{SiMe}_3)_2$ in THF produced a series of lanthanide (III) mono- or di-substituted bis(trimethylsilyl)amido chloride complexes. We found

that reactions of the monosubstituted silylamido complexes **5–7** with two equiv. of $\text{LiN}(\text{SiMe}_3)_2$ could easily lead to the formation of the disubstituted ones **1–3** and **9**. Compounds **1–9** were characterized by melting point determination, elemental analysis and IR spectra and **1–3**, **5**, **6** and **8** were structurally determined by X-ray crystallography. The structures of these compounds are chloride-bridged dimers in which Ln metals in **1–3** display a distorted trigonal bipyramidal coordination geometry while those in **5**, **6** and **8** a distorted octahedral coordination geometry. Moreover, these complexes showed catalytic activity for the ring-opening polymerization of ϵ -caprolactone. As the disubstituted compounds **1–3** and **9** have more open coordination environment around the metal atoms than **4–8**, they showed better catalytic activity than the monosubstituted complexes **4–8**. In addition, it should be noted that the mono- or di-substituted bis(trimethylsilyl)amido complexes may be good precursors for the preparation of other novel lanthanide compounds. For example, lanthanide thiolate complexes $[(\text{Me}_3\text{Si})_2\text{N}]_2\text{Ln}(\text{SBu-}t)]_2$ (Ln = Gd, Yb) [38] could be prepared by reactions of $[(\mu\text{-Cl})\text{Ln}\{\text{N}(\text{SiMe}_3)_2\}_2(\text{THF})]_2$ with $\text{Li}(\text{SBu-}t)$. Therefore, a systematic study on the reactions of **1–9** with various thiolates is worth to make and is actually ongoing in our laboratory.

4. Experimental

4.1. General

All manipulations were carried out under argon using standard Schlenk-techniques. All solvents were refluxed and distilled over sodium benzophenone ketyl under argon prior to use. $\text{LiN}(\text{SiMe}_3)_2$ [10] and LnCl_3 [39] were prepared according to published procedures. ϵ -caprolac-

tone, purchased from ACROS Com., was dried by stirring with CaH_2 for 8 days, and then distilled under reduced pressure. Elemental analyses data were obtained on a Carlo-Erbo CHNO-S Elemental Analyzer. The IR spectra (KBr, disc) were recorded on a Nicolet Magna-IR550 FT-IR spectrometer ($4000\text{--}400\text{ cm}^{-1}$). The uncorrected melting points were determined in argon-sealed capillary tubes on a Mel-Temo II apparatus. Molecular weight and molecular weight distributions were determined against polystyrene standard by gel permeation chromatography (GPC) on a Waters 1515 apparatus with three HR columns (HR-1, HR-2 and HR-4); THF was used as an eluent.

4.2. Syntheses

4.2.1. Preparation of **1**

To a 100 mL Schlenk flask containing a suspension of anhydrous NdCl_3 (1.087 g, 4.39 mmol) in 40 mL THF at 193 K was added freshly prepared anhydrous $\text{LiN}(\text{SiMe}_3)_2$ solid (1.348 g, 8.07 mmol). The reaction mixture was allowed to slowly warm up to room temperature by removing the cooling bath. After it was stirred overnight, the resulting clear blue solution was reduced to dryness under vacuum. The residual was extracted with 50 mL of hot *n*-hexane and the resulting lithium chloride was filtered off via cannula. The filtrate was concentrated to ca. 20 mL, and blue crystalline solid of $[\{((\text{Me}_3\text{Si})_2\text{N})_2\text{Nd}(\mu'\text{-Cl})\text{Li}(\text{THF})_3\}(\mu\text{-Cl})]_2$ (**1**) was formed upon standing it at room temperature for several days. Yield: 2.05 g, (67%), m.p. 372–374 K. Calc. for $\text{C}_{48}\text{H}_{120}\text{Cl}_4\text{Li}_2\text{N}_4\text{Nd}_2\text{O}_6\text{Si}_8$: C, 37.97; H, 7.97; N, 3.69. Found: C, 38.05; H, 8.01; N, 3.73%. IR (KBr disc): 2881 (s), 1628 (m), 1408 (m), 1253 (s), 1047 (s), 843 (s), 618 (w) cm^{-1} .

4.2.2. Preparation of **2**

To a 100 mL Schlenk flask containing a suspension of anhydrous EuCl_3 (1.87 g, 7.23 mmol) in 40 mL of THF was added anhydrous $\text{LiN}(\text{SiMe}_3)_2$ solid (2.41 g, 14.46 mmol) at room temperature. The resulting clear red solution was stirred overnight. After the solvent was removed in vacuo, the crude product was extracted with hot *n*-hexane and the insoluble LiCl was filtered off. The filtrate was kept at 295 K for two days and slightly yellow crystalline solids of red crystals of $[\{((\text{Me}_3\text{Si})_2\text{N})_2\text{Eu}(\mu'\text{-Cl})\text{Li}(\text{THF})_2\}(\mu_3\text{-Cl})]_2$ (**2**). Yield: 3.66 g (73%), m.p. 368–370 K. Anal. Calc for $\text{C}_{40}\text{H}_{104}\text{Cl}_4\text{Eu}_2\text{Li}_2\text{N}_4\text{O}_4\text{Si}_8$: C, 34.57; H, 7.54; N, 4.03. Found C, 34.73; H, 7.64; N, 4.12%. IR (KBr disc): 2883 (s), 1625 (m), 1407 (m), 1251 (s), 1046 (s), 841(m), 619 (w) cm^{-1} .

4.2.3. Preparation of **3**

The similar reaction of anhydrous HoCl_3 (0.699 g, 2.57 mmol) with $\text{LiN}(\text{SiMe}_3)_2$ (0.822 g, 4.92 mmol) followed by a similar work-up to that used in the isolation

of **2** afforded colorless crystals of $[\{((\text{Me}_3\text{Si})_2\text{N})_2\text{Ho}(\mu'\text{-Cl})\text{Li}(\text{THF})_2\}(\mu_3\text{-Cl})]_2$ (**3**). Yield: 0.92 g (53%), m.p. 374–376 K. Anal. Calc. for $\text{C}_{40}\text{H}_{104}\text{Cl}_4\text{Ho}_2\text{Li}_2\text{N}_4\text{O}_4\text{Si}_8$: C, 33.94; H, 7.41; N 3.96. Found C, 34.03; H, 7.74; N, 4.02%. IR (KBr disk): 2881 (s), 1622 (m), 1409 (m), 1253 (s), 1046 (s), 840 (m), 617 (w) cm^{-1} .

4.2.4. Preparation of **4**

A solution of $\text{LiN}(\text{SiMe}_3)_2$ (0.444 g, 2.66 mmol) in THF (20 mL) was added dropwise to a suspension of anhydrous NdCl_3 (0.71 g, 2.87 mmol) in 15 mL THF. After stirring for 10 h at room temperature, all volatile species was removed under vacuum and the crude product was extracted with hot toluene and the insoluble LiCl was filtered off. The filtrate was kept at 275 K for several day and blue crystals of $[\{(\text{Me}_3\text{Si})_2\text{NNd}(\mu'\text{-Cl})_2\text{Li}(\text{THF})_2\}(\mu\text{-Cl})]_2$ (**4**) were formed. Yield: 0.79 g (41%), m.p. 355–358 K. Anal. Calc. for $\text{C}_{36}\text{H}_{84}\text{Cl}_6\text{Nd}_2\text{Li}_2\text{N}_2\text{O}_6\text{Si}_4$: C, 34.09; H, 6.67; N, 2.21. Found: C, 33.87; H, 6.79; N, 2.53%. IR (KBr disc): 2951 (s), 1463 (s), 1375 (w), 1349 (s), 1261 (m), 1183 (m), 1050 (s), 939 (s), 695 (w), 614 (w), 410 (w) cm^{-1} .

4.2.5. Preparation of **5**

The similar reaction of anhydrous SmCl_3 (0.822 g, 3.2 mmol) with $\text{LiN}(\text{SiMe}_3)_2$ (0.7 g, 4 mmol) in THF followed by a similar work-up to that used in the isolation of **4** afforded pale yellow crystals of $[\{(\text{Me}_3\text{Si})_2\text{NSm}(\mu'\text{-Cl})_2\text{Li}(\text{THF})_2\}(\mu\text{-Cl})]_2$ (**5**). Yield: 0.82 g (45%), m.p. 360–362 K. Anal. Calc. for $\text{C}_{36}\text{H}_{84}\text{Cl}_6\text{Li}_2\text{N}_2\text{O}_6\text{Si}_4\text{Sm}_2$: C, 33.76; H, 6.61; N, 2.18. Found: C, 33.58; H, 6.72; N, 2.19%. IR (KBr disc): 2955 (s), 1460 (s), 1372 (w), 1347 (m), 1256 (m), 1179 (m), 1048 (s), 942 (s), 699 (w), 611 (m), 404 (w) cm^{-1} .

4.2.6. Preparation of **6**

The similar reaction of anhydrous EuCl_3 (0.827 g, 3.2 mmol) with $\text{LiN}(\text{SiMe}_3)_2$ (0.501 g, 3 mmol) in THF followed by a similar work-up to that used in the isolation of **4** afforded red crystals of $[\{(\text{Me}_3\text{Si})_2\text{NEu}(\mu'\text{-Cl})_2\text{Li}(\text{THF})_2\}(\mu\text{-Cl})]_2$ (**6**). Yield: 0.79 g (53%), m.p. 365–367 K. Anal. Calc. for $\text{C}_{36}\text{H}_{84}\text{Cl}_6\text{Eu}_2\text{Li}_2\text{N}_2\text{O}_6\text{Si}_4$: C, 33.67; H, 6.59; N, 2.18. Found: C, 33.57; H, 6.71; N, 2.24%. IR (KBr disc): 2953 (s), 1461 (s), 1374 (w), 1344 (m), 1258 (m), 1181 (m), 1051 (s), 944 (s), 701 (w), 613 (m), 406 (w) cm^{-1} .

4.2.7. Preparation of **7**

The similar reaction of anhydrous HoCl_3 (0.85 g, 3.13 mmol) with $\text{LiN}(\text{SiMe}_3)_2$ (0.688 g, 4.12 mmol) in THF followed by a similar work-up to that used in the isolation of **4** afforded colorless crystals of $[\{(\text{Me}_3\text{Si})_2\text{NHo}(\mu'\text{-Cl})_2\text{Li}(\text{THF})_2\}(\mu\text{-Cl})]_2$ (**7**). Yield: 0.79 g (47%), m.p. 359–362 K. Anal. Calc. for $\text{C}_{36}\text{H}_{84}\text{Cl}_6\text{Ho}_2\text{Li}_2\text{N}_2\text{O}_6\text{Si}_4$: C, 33.10; H, 6.46; N, 2.14. Found: C, 33.36; H, 6.77; N, 2.33%. IR (KBr disc): 2961 (s), 1465 (s), 1368

Table 5
Summary of the crystal data for the structures of **1**, **2**, **3**, **5**, **6**, **8**

	1	2	3	5	6	8
Empirical formula	C ₄₈ H ₁₂₀ Cl ₄ Li ₂ N ₄ Nd ₂ O ₄ Si ₈	C ₄₀ H ₁₀₄ Cl ₄ Eu ₂ Li ₂ N ₄ O ₄ Si ₈	C ₄₀ H ₁₀₄ Cl ₄ Ho ₂ Li ₂ N ₄ O ₄ Si ₈	C ₃₆ H ₈₄ Cl ₆ Li ₂ N ₂ O ₆ Si ₄ Sm ₂	C ₃₆ H ₈₄ Cl ₆ Eu ₂ Li ₂ N ₂ O ₆ Si ₄	C ₃₆ H ₈₄ Cl ₆ Li ₂ N ₂ O ₆ Si ₄ Yb ₂
F_w	1518.36	1389.61	1415.53	1280.81	1283.93	1326.09
Crystal system	Triclinic	triclinic	Monoclinic	Triclinic	Triclinic	Triclinic
Space group	$P\bar{1}$ (No. 2)	$P\bar{1}$ (No. 2)	$P2_1/n$ (No. 14)	$P\bar{1}$ (No. 2)	$P\bar{1}$ (No. 2)	$P\bar{1}$ (No. 2)
a (Å)	12.195(5)	12.227(4)	13.150(4)	9.458(3)	9.4639(6)	9.4890(11)
b (Å)	13.110(5)	12.361(4)	19.747(6)	12.605(4)	12.5795(10)	12.490(2)
c (Å)	15.053(6)	13.328(5)	13.407(4)	13.104(4)	13.0875(9)	12.986(2)
α (°)	101.2919(11)	72.699(10)	90	82.297(11)	82.327(5)	82.189(11)
β (°)	106.858(3)	79.529(10)	93.728(4)	74.109(8)	74.086(5)	73.393(8)
γ (°)	114.643(3)	64.675(10)	90	77.724(10)	77.760(5)	77.522(10)
V (Å ³)	1949.7(13)	1734.9(10)	3474.1(18)	1463.4(8)	1459.6(2)	1435.5(4)
D_c (g cm ^{−3})	1.293	1.330	1.353	1.453	1.461	1.534
Z	1	1	2	1	1	1
$F(000)$	790	716	724	650	652	666
$2\theta_{\max}$ (°)	55.0	55.0	55.0	55.0	50.70	55.0
μ (cm ^{−1})	1.615	2.117	2.589	2.383	2.522	3.637
Reflections ($I > 3.00\sigma(I)$)	6160	7104	5693	5824	4432	5616
Parameters	394	341	341	304	304	304
R^a	0.0230	0.0280	0.0540	0.0310	0.0400	0.0400
R_w^b	0.0250	0.0430	0.0620	0.0440	0.0500	0.0500
Goodness-of-fit ^c	0.947	0.996	1.038	1.016	1.036	1.019
ρ_{\max} (e Å ^{−3})	0.95	1.47	1.31	1.25	1.50	0.88
ρ_{\min} (e Å ^{−3})	−0.60	−0.91	−0.99	−1.54	−1.54	−1.17

^a $R = \sum ||F_o| - |F_c|| / \sum |F_o|$.

^b $R_w = \{ \sum (|F_o| - |F_c|)^2 / \sum w |F_o|^2 \}^{1/2}$.

^c GOF = $\{ \sum w (|F_o| - |F_c|)^2 / (M - N) \}^{1/2}$, where M is the number of reflections and N is the number of parameters.

(w), 1356 (m), 1260 (m), 1175 (m), 1053 (s), 948 (s), 705 (w), 617 (w), 405 (w) cm^{-1} .

4.2.8. Preparation of **8**

The similar reaction of anhydrous YbCl_3 (0.721 g, 2.58 mmol) with $\text{LiN}(\text{SiMe}_3)_2$ (0.441 g, 2.64 mmol) in THF followed by a similar work-up to that used in the isolation of **4** afforded pale yellow crystals of $[(\text{Me}_3\text{Si})_2\text{NYb}(\mu\text{-Cl})_2\text{Li}(\text{THF})_2](\mu\text{-Cl})_2$ (**8**). Yield: 0.67 g (39%), m.p. 372–373 K. Anal. Calc. for $\text{C}_{36}\text{H}_{84}\text{Cl}_6\text{Li}_2\text{N}_2\text{O}_6\text{Si}_4\text{Yb}_2$: C, 32.61; H, 6.38; N, 2.11. Found: C, 33.01; H, 6.12; N, 2.35%. IR (KBr disk): 2953 (s), 1465 (s), 1369 (w), 1352 (m), 1255 (m), 1181 (m), 1052 (s), 946 (s), 701 (w), 608 (m), 403 (w) cm^{-1} .

4.2.9. Reaction of **4** with two equiv. $\text{LiN}(\text{SiMe}_3)_2$

A solution of $\text{LiN}(\text{SiMe}_3)_2$ (0.316 g, 1.89 mmol) in THF (20 mL) was added dropwise to a clear solution of **4** (1.2 g, 0.95 mmol) in 15 mL THF. Complex **1** was obtained (0.87 g, 61%) in a similar workup to that used in a similar work-up to that used in the isolation of **1**.

4.2.10. Reaction of **5** with two equiv. $\text{LiN}(\text{SiMe}_3)_2$

A solution of $\text{LiN}(\text{SiMe}_3)_2$ (0.35 g, 2.09 mmol) in THF (15 mL) was added dropwise to a clear solution of **5** (1.34 g, 1.05 mmol) in 15 mL THF. $[(\text{Me}_3\text{Si})_2\text{N})_2\text{Sm}(\mu\text{-Cl})\text{Li}(\text{THF})_3](\mu\text{-Cl})_2$ (**9**) was obtained in a similar workup to that used in a similar work-up to that used in the isolation of **1**. Yield: 1.10 g (69%), m.p. 365–367 K. Anal. Calc for $\text{C}_{48}\text{H}_{120}\text{Cl}_4\text{Li}_2\text{N}_4\text{Sm}_2\text{O}_6\text{Si}_8$: C, 37.67; H, 7.90; N, 3.66. Found C, 37.67; H, 7.90; N, 3.66%. IR (KBr disk): 2998 (s), 2885 (s), 1621 (m), 1410 (w), 1248 (s), 1049 (s), 838 (m), 621 (m) cm^{-1} .

4.2.11. Reaction of **6** with two equiv. $\text{LiN}(\text{SiMe}_3)_2$

A solution of $\text{LiN}(\text{SiMe}_3)_2$ (0.30 g, 1.8 mmol) in THF (15 mL) was added dropwise to a clear solution of **6** (1.15 g, 0.9 mmol) in 15 mL THF. Complex **2** was obtained (0.812 g, 65%) in a similar workup to that used in a similar work-up to that used in the isolation of **1**.

4.2.12. Reaction of **7** with two equiv. $\text{LiN}(\text{SiMe}_3)_2$

A solution of $\text{LiN}(\text{SiMe}_3)_2$ (0.23 g, 1.38 mmol) in THF (15 mL) was added dropwise to a clear solution of **7** (0.916 g, 0.7 mmol) in 15 mL THF. Complex **3** was obtained (0.55 g, 56%) in a similar workup to that used in a similar work-up to that used in the isolation of **1**.

4.2.13. Typical procedure for the ROP of ϵ -caprolactone

The procedures for the polymerization of ϵ -caprolactone are the same (Table 4). And a typical polymerization reaction is given below (entry 1 and 5, Table 4). A 50 mL Schlenk flask equipped with a magnetic stir bar was charged with 8 mL toluene and 0.0141 g of **1**.

The clear solution was added 1.5 mL ϵ -caprolactone via a syringe. The contents of the flask were stirred vigorously at 298 K, and quenched by the addition of 1 M HCl in EtOH. The solution was then poured into 50 mL of petroleum ether to precipitate the white oligomer. After being washed with methanol for three times, the oligomer was collected and dried in vacuo.

4.2.14. X-ray diffraction crystallography

All measurements were made on a Rigaku Mercury CCD X-ray diffractometer (3 kV, sealed tube) at 193 K by using graphite monochromated Mo $\text{K}\alpha$ ($\lambda = 0.71070$ Å). X-ray quality crystals of **1**, **2**, **3**, **5**, **6**, **8** were obtained directly from the above preparations. A light-blue chunk of **1** with dimensions $0.55 \times 0.45 \times 0.55$ mm, a red block of **2** with dimensions $0.20 \times 0.40 \times 0.55$ mm, a colorless block of **3** with $0.35 \times 0.55 \times 0.45$ mm, a colorless block of **5** with $0.16 \times 0.50 \times 0.45$ mm, a red block of **6** with $0.18 \times 0.80 \times 0.40$ mm, a pale yellow block of **8** with $0.14 \times 0.80 \times 0.24$ mm were mounted in a sealed capillary. Diffraction data were collected at ω – 2θ mode with a detector distance of 54.69 mm for **1**, 54.73 mm for **2**, 44.51 mm for **3**, 44.49 mm for **5**, 34.53 mm for **6**, 34.58 mm for **8** mm to the crystals. The collected data were reduced by using the program CrystalClear (Rigaku and MSC, Ver.1.3, 2001), and an empirical absorption correction was applied which resulted in transmission factors ranging from 0.428 to 0.484 for **1**, from 0.377 to 0.655 for **2**, from 0.193 to 0.404 for **3**, from 0.318 to 0.683 for **5**, from 0.311 to 0.636 for **6**, from 0.365 to 0.601 for **8**. The reflection data were also corrected for Lorentz and polarization effects.

The structures of **1**, **2**, **3**, **5**, **6** and **8** were solved by direct methods [40] (**1**, **3**, **6** and **8**) or heavy-atom Patterson method [41] (**2** and **7**) and refined by full matrix least-squares on F [42]. All the non-hydrogen atoms were refined anisotropically. All hydrogen atoms were introduced at the calculated positions and included in the structure-factor calculations. All the calculations were performed on a Dell workstation using the Crystal-Structure crystallographic software package (Rigaku and MSC, Ver.3.60, 2004). Crystal and data collection parameters for **1**, **2**, **3**, **5**, **6** and **8** are summarized in Table 5.

Acknowledgements

This work was supported by the Chinese National Science Foundation (No. 20271036), the NSF of the Education Committee of Jiangsu Province (No. 02KJB150001), the State Key Laboratory of Organometallic Chemistry, Shanghai Institute of Organic Chemistry, Chinese Academy of Sciences (No. 04-33), and Key Laboratory of Organic Synthesis of Jiangsu Province (No. JSK001) in China.

Appendix A. Supplementary material

Crystallographic data for the structural analyses have been deposited with Cambridge Crystallographic Data Centre, CCDC reference numbers 232609 (**1**), 232610 (**2**), 232611 (**3**), 232612 (**5**), 243037 (**6**) and 232613 (**8**). Copies of this information may be obtained free of charge from The Director, CCDC, 12 Union Road, Cambridge CB2 1E2, UK (fax: +44-1223-336033; deposit@ccdc.cam.ac.uk. or www.ccdc.cam.ac.uk). Supplementary data associated with this article can be found, in the online version at doi:10.1016/j.jorganchem.2004.07.044.

References

- [1] (a) R. Anwender, *Top. Curr. Chem.* 179 (1996) 33–112; (b) M.T. Gamer, S. Dehnen, P.W. Roesky, *Organometallic* 20 (2001) 4230–4236; (c) B.H. Koo, Y. Byun, E. Hong, Y. Kim, Y. Do, *Chem. Commun.* (1998) 1227–1228; (d) R. Anwender, O. Runte, J. Eppinger, G. Gerstberger, E. Herdtweck, M. Spiegler, *J. Chem. Soc., Dalton Trans.* (1998) 847–858; (e) P.W. Roesky, *Organometallics* 21 (2002) 4756–4761; (f) G.B. Deacon, G.D. Fallon, C.M. Forsyth, H. Schumann, R. Weimann, *Chem. Ber.* 130 (1997) 409–415; (g) R. Kempe, *Angew. Chem., Int. Ed.* 39 (2000) 468–493; (h) R. Kempe, H. Noss, H. Fuhrmann, *Chem. Eur. J.* 7 (2001) 1630–1636; (i) S.C.F. Kui, H.W. Li, H.K. Lee, *Inorg. Chem.* 42 (2003) 2824–2826.
- [2] D.C. Bradley, H. Chudzynska, M.B. Hursthouse, M. Motevalli, *Polyhedron* 10 (1991) 1049–1059.
- [3] K.G. Caulton, L.G. Hubert-Pfalzgraf, *Chem. Rev.* 90 (1990) 969–995.
- [4] B. Cetinkaya, P.B. Hitchcock, M.F. Lappert, R.G. Smith, *J. Chem. Soc., Chem. Commun.* (1992) 932–934.
- [5] W.A. Herrmann, J. Eppinger, M. Spiegler, O. Runte, R. Anwender, *Organometallics* 16 (1997) 1813–1815.
- [6] J. Eppinger, M. Spiegler, W. Heringer, W.A. Herrmann, R. Anwender, *J. Am. Chem. Soc.* 122 (2000) 3080–3096.
- [7] A.K. Dash, A. Razavi, A. Mortreux, C.W. Lehmann, J.F. Carpentier, *Organometallics* 21 (2002) 3238–3249.
- [8] (a) M.A. Giardello, V.P. Conticello, L. Brard, M.R. Gagné, T.J. Marks, *J. Am. Chem. Soc.* 116 (1994) 10241–10254; (b) M.A. Giardello, Y. Yamamoto, L. Brard, T.J. Marks, *J. Am. Chem. Soc.* 117 (1995) 3276–3277.
- [9] A.C. Greenwald, W.S. Rees Jr., U.W. Lay, in: G.S. Pomrenke, P.B. Klein, D.W. Langer (Eds.), *Rare Earth Doped Semiconductors*, MRS, Pittsburgh, PA, 1993.
- [10] D.C. Bradley, J.S. Ghotra, F.A. Hart, *J. Chem. Soc., Dalton Trans.* (1973) 1021–1023.
- [11] (a) Z. Hou, Y. Wakatsuki, *Coord. Chem. Rev.* 231 (2002) 1–22; (b) R.A. Andersen, D.H. Templeton, A. Zalkin, *Inorg. Chem.* 17 (1978) 2317–2319; (c) J.S. Ghotra, M.B. Hursthouse, A.J. Welch, *J. Chem. Soc., Chem. Commun.* (1973) 669–670; (d) P.G. Eller, D.C. Bradley, M.B. Hursthouse, D.W. Meek, *Coord. Chem. Rev.* 24 (1977) 1–95; (e) W.S. Rees Jr., O. Just, D.S. Van Derreer, *J. Mater. Chem.* 9 (1999) 249–252.
- [12] (a) F.T. Edelman, A. Steiner, D. Stalke, J.W. Gilje, S. Jagner, M. Håkansson, *Polyhedron* 13 (1994) 539–546; (b) S.L. Zhou, S.W. Wang, G.S. Yang, X.Y. Liu, E.H. Sheng, K.H. Zhang, L. Cheng, Z.X. Huang, *Polyhedron* 22 (2003) 1019–1024; (c) E.H. Sheng, S.W. Wang, G.S. Yang, S.L. Zhou, L. Cheng, K.H. Zhang, Z.X. Huang, *Organometallics* 22 (2003) 684.
- [13] B. Martin Vaca, A. Dumitrescu, H. Gornitzka, D. Bourissow, G. Bertrand, *J. Organomet. Chem.* 682 (2003) 263–266.
- [14] D.J. Berg, R.A.L. Gendron, *Can. J. Chem.* 78 (2000) 454.
- [15] H.C. Aspinall, D.C. Bradley, M.B. Hursthouse, K.D. Sales, N.P.C. Walker, B. Hussain, *J. Chem. Soc., Dalton Trans.* (1989) 623–626.
- [16] W.J. Evans, D.K. Drummond, H.M. Zhang, J.L. Atwood, *Inorg. Chem.* 27 (1988) 575–579.
- [17] T.D. Tilley, R.A. Andersen, A. Zalkin, *Inorg. Chem.* 23 (1984) 2271–2276.
- [18] P. Dubois, C. Jacobs, R. Jerome, P. Teyssie, *Macromolecules* 24 (1991) 2266–2270.
- [19] A.J. Nijenhuis, D.W. Grijpma, A.J. Pennings, *Macromolecules* 25 (1992) 6419–6424.
- [20] A. Duda, S. Penczek, *Macromolecules* 23 (1990) 1636–1639.
- [21] D.B. Johns, R.W. Lenz, A. Luick, in: K.J. Ivin, T. Saegusa (Eds.), *Ring-Opening Polymerization*, Vol. 1, Elsevier Applied Science Publishers, London, Great Britain, 1984, pp. 461–521 (Chapter 7).
- [22] S.J. McLain, N.E. Drysdale, WO 9105001. (*Chem. Abstr.*) 115 (1993) 715.
- [23] W.M. Stevels, M.J.K. Ankoné, P.J. Dijkstra, J. Feijen, *Macromolecules* 29 (1996) 8296–8303.
- [24] W.M. Stevels, M.J.K. Ankone, P.J. Dijkstra, J. Feijen, *Macromol. Chem. Phys.* 196 (1995) 1153–1161.
- [25] M. Yamashita, Y. Takemoto, E. Ihara, H. Yasuda, *Macromolecules* 29 (1996) 1798–1806.
- [26] (a) K.C. Hultsch, T.P. Spaniol, J. Okuda, *Organometallics* 16 (1997) 4845–4846; (b) E. Martin, P. Dubois, R. Jérôme, *Macromolecules* 33 (2000) 1530–1535.
- [27] (a) W.J. Evans, H. Katsumata, *Macromolecules* 27 (1994) 2330–2332; (b) S. Agarwal, C. Mast, S. Anfang, M. Karl, K. Dehnicke, A. Greiner, *Polym. Prepr. (Am. Chem. Soc., Div. Polym. Chem.)* 39 (1998) 414–415; (c) S. Agarwal, M. Karl, S. Anfang, K. Dehnicke, A. Greiner, *Polym. Prepr. (Am. Chem. Soc., Div. Polym. Chem.)* 39 (1998) 361–362.
- [28] P.W. Roesky, M.R. Burystein, *Inorg. Chem.* 38 (1999) 5629–5632.
- [29] J.E. Cosgriff, G.B. Deacon, G.D. Fallon, B.M. Gatehouse, H. Schumann, R. Weimann, *Chem. Ber.* 129 (1996) 953–958.
- [30] W.J. Evans, J.L. Shreeve, J.W. Ziller, *Organometallics* 13 (1994) 731–733.
- [31] O. Just, W.S. Rees Jr., *Inorg. Chem.* 40 (2001) 1751–1755.
- [32] Z.H. Wu, Z. Xu, X.Z. You, H.Q. Wang, X.G. Zhou, *Polyhedron* 12 (1993) 677–681.
- [33] R.K. Minhas, Y. Ma, J. Song, S. Gambarotta, *Inorg. Chem.* 35 (1996) 1866–1873.
- [34] W.J. Evans, R.A. Keyer, J.W. Ziller, *Organometallics* 12 (1993) 2618–2633.
- [35] M.A. Giardello, V.P. Conticello, L. Brard, M. Sabat, A. L. Rheingold, C.L. Stern, T.J. Marks, *J. Am. Chem. Soc.* 116 (1994) 10212–10240.
- [36] M. Brewer, J. Lee, J.G. Brennan, *Inorg. Chem.* 34 (1995) 5919.
- [37] W.M. Stevels, M.J.K. Ankoné, P.J. Dijkstra, J. Feijen, *Macromolecules* 29 (1996) 8296–8303.
- [38] H.C. Aspinall, D.C. Bradley, M.B. Hursthouse, K.D. Sales, N.P.C. Walker, *J. Chem. Soc., Chem. Commun.* (1985) 1585–1586.

- [39] M.D. Taylor, C.P. Carter, *J. Inorg. Nucl. Chem.* 24 (1962) 387–391.
- [40] G.M. Sheldrick, SHELXS-97: Program for the Solution of Crystal Structure, University of Göttingen, Germany, 1997.
- [41] P.T. Beurskens, G. Admiral, G. Beurskens, W.P. Bosman, S. Garcia-Granda, R.O. Gould, J.M.M. Smits, C. Smykalla, PATTY: The DIRDIF program system, Technical, Report of the Crystallography Laboratory, University of Nijmegen, The Netherlands, 1992.
- [42] P.T. Beurskens, G. Admiral, G. Beurskens, W.P. Bosman, R. de Gelder, R. Israel, J.M.M. Smits, DIRDIF-94: The DIRDIF-94 program system, Technical, Report of the Crystallography Laboratory, University of Nijmegen, The Netherlands, 1992.